

Quantum Information Scrambling Through a High-Complexity Operator Mapping

Xiaopeng Li,^{1,2} Guanyu Zhu,³ Muxin Han,^{4,5} and Xin Wang⁶

¹*State Key Laboratory of Surface Physics, Institute of Nanoelectronics and Quantum Computing, and Department of Physics, Fudan University, Shanghai 200433, China*

²*Collaborative Innovation Center of Advanced Microstructures, Nanjing 210093, China**

³*Joint Quantum Institute, NIST/University of Maryland, College Park, Maryland 20742, USA*

⁴*Department of Physics, Florida Atlantic University, 777 Glades Road, Boca Raton, FL 33431, USA*

⁵*Institut für Quantengravitation, Universität Erlangen-Nürnberg, Staudtstr. 7/B2, 91058 Erlangen, Germany*

⁶*Department of Physics, City University of Hong Kong,*

Tat Chee Avenue, Kowloon, Hong Kong SAR, China,

and City University of Hong Kong Shenzhen Research Institute, Shenzhen, Guangdong 518057, China

(Dated: August 7, 2022)

Quantum information scrambling has attracted much attention amid the effort to reconcile the conflict between quantum-mechanical unitarity and the thermalization-irreversibility in many-body systems. Here we propose an unconventional mechanism to generate quantum information scrambling through a high-complexity mapping from logical to physical degrees-of-freedom that hides the logical information into non-separable many-body-correlations. Corresponding to this mapping, we develop an algorithm to efficiently sample a Slater-determinant wave-function and compute all physical observables in dynamics with a polynomial cost in system-size. The system shows information scrambling in the quantum many-body Hilbert space characterized by the spreading of Hamming-distance. We establish that the operator-mapping enabled growth in out-of-time-order-correlator exhibits exponential-scrambling behaviour. Our sampling-algorithm is expected to be applicable in accelerating quantum chemistry calculations and building classically-simulatable quantum-machine-learning architectures that exploit quantum-interference effects. We expect the quantum information-hiding mapping approach to shed light on the understanding of fundamental connections among computational complexity and information scrambling.

Introduction.— Recent developments in engineering synthetic quantum devices have achieved unprecedented controllability over a wide range of quantum degrees of freedom [1–4]. Theoretically, it has been realized that there is an intricate difference between few- and many- qubit systems—a few-qubit system undergoing unitary evolution is easily reversible by a quantum circuit, whereas the reverse for many qubits is in general very difficult or practically impossible due to quantum thermalization despite of unitarity [5–10]. This conflict between unitarity and irreversibility with many qubits undermines our fundamental understanding of quantum thermalization in a closed quantum system. To reconcile the conflict, the eigenstate thermalization hypothesis has been formulated theoretically [5, 6] and confirmed numerically [11]. Nevertheless, the microscopic mechanism of the thermalization still remains mysterious. Amid the fast-growing research interests on synthetic quantum systems for the purposes of quantum information processing and beyond, a thorough understanding of this problem is key for the field to advance [12].

The problem of many-body unitarity also emerges in modeling quantum effects of black holes [13]. The black hole information and the recent firewall paradox

have received enormous research interests in the last few years [14–22]. One puzzle is that the thermal nature of black-hole evaporation process through Hawking radiation obtained from semi-classical calculations is inconsistent with a full quantum mechanical description.

In both contexts of quantum thermalization and black-hole information paradox, researchers are now approaching a consensus that understanding how quantum information scrambles is crucial to resolve the issues in quantum many-body unitarity [23]. In connecting quantum microscopic degrees of freedom to large-scale classical (or semiclassical) physical processes, the interplay of quantum chaos [23], operator growth [22, 24], and computational complexity [25–27] is of deep fundamental interest. Recent developments following the idea of the holographic anti-de Sitter/conformal field theory correspondence [28] have explored the quantum chaotic aspect through the 0+1 dimensional Sachdev-Ye-Kitaev (SYK) model [29, 30] and its variants [15, 20–22], whose out-of-time-order-correlators (OTOC) are analytically solvable at large-N limit. However, other equally important aspects such as operator growth, computational complexity, and emergence of (semi-)classical descriptions are not well-captured by the previously studied analytically-solvable models [22, 29, 30], deserving novel theoretical ideas for further progress [25, 26].

Here we propose an unconventional approach for

* xiaopeng_li@fudan.edu.cn

quantum information scrambling by applying a high complexity mapping. In our proposed mechanism, despite that the quantum state follows integrable unitary evolution, quantum information is gradually lost in a physical setting, morphing into non-separable many-body correlations because of the high complexity of the mapping between integrals of motion and physical observables in the system. This mechanism is demonstrated by a specific carefully-designed operator mapping in a $1 + 1$ dimensional setting. We show that the system exhibits information scrambling in the exponentially-sized Hilbert space. This dynamical process is quantified by a Hamming distance [31]. Corresponding to the mapping, we develop an algorithm and show the system is efficiently tractable on a classical computer—the time-cost scales polynomially in the system-size. At late-time quantum dynamics, we find a classical diffusion description emerges out of the microscopic quantum degrees of freedom. In principle the mapping-complexity in our proposed mechanism can be generalized to more generic cases, which we expect to open up a wide window to investigate the fundamental interplay of computational complexity, quantum thermalization and information scrambling. A byproduct worth remarking is that the sampling-algorithm developed here is expected to be useful in accelerating quantum chemistry calculations and building classically-simulatable quantum-machine-learning architectures.

Quantum information scrambling through a high-complexity operator-mapping.— For a generic quantum system the time evolution of a physical observable \mathcal{O} is described by the expectation value of the Heisenberg operator $\mathcal{O}(t) = e^{iHt} \mathcal{O} e^{-iHt}$, with H the system Hamiltonian. Considering a quantum state $|\Psi\rangle$ with information encoded by a set of few-body observables as $\mathcal{O}_\alpha|\Psi\rangle = \lambda_\alpha|\Psi\rangle$ —for example these operators could be local pauli operators or stabilizers—its quantum evolution is deterministically given by $\mathcal{O}_\alpha(-t)|\Psi(t)\rangle = \lambda_\alpha|\Psi(t)\rangle$. Through this dynamical process the information becomes hidden into $\mathcal{O}_\alpha(-t)$, which in general involve highly nonlocal many-body operators [22, 24, 32, 33]. Tracking the mapping $\{\mathcal{O}_\alpha\} \mapsto \{\mathcal{O}_\alpha(-t)\}$ for a generic Hamiltonian is exponentially complex, making the extraction of quantum information after long-time evolution practically impossible, i.e., quantum information scrambles under the time evolution. The scrambling process can thus be treated as quantum information initiated in few-body degrees of freedom hidden into non-separable many-body correlations through a high-complexity mapping. Mathematically, we can define a logical basis that stores the quantum information according to the eigenbasis of $\mathcal{O}_\alpha(-t)$, and study the information scrambling in the physical degrees of freedom. The information scrambling is thus generically basis-

dependent and as a result the intrinsic physics solely relies on the mapping between logical and physical basis (see an illustration in TABLE I). It is worth emphasizing here that this aspect is not captured by the well-studied SYK model [29, 30] or its variants despite they are analytically solvable.

It is evident that the capability of the mapping to build in non-separable many-body correlations is required to connect the information-preserving logical basis to the scrambling physical basis, but it is unclear whether the mapping having an exponential complexity is also necessary or not. Finding a relatively lower-complexity mapping from few- to many-body operators that still causes information scrambling is not only of fundamental interest but would also assist in constructing exact models for nontrivial quantum many-body dynamics. In constructing such a mapping, we require that (i) the mapping has to be complicated enough to enable scrambling, (ii) the mapping is numerically tractable with low-cost, or more specifically having polynomial computational complexity, and (iii) the locality of the quantum evolution must be respected by the mapping—the dynamics in both logical and physical basis should be local. We remark here that the Jordan Wigner [34] or the Clifford gate unitary mapping [18] does not satisfy these requirements. In the following, we devise a suitable mapping based on spin-1/2 qubits. We emphasize that the proposed theoretical ideas are rather generalizable than restricted to the particular mapping.

Consider a one-dimensional spin chain, $\sigma_j^{x,y,z}$, with the site index $j \in [1, L]$. We assume that the total spin S_z component is conserved, and shall work in the Hilbert space sector having $\sum_{j=1}^L \sigma_j^z / 2 = S_z$. This S_z conservation holds in the quantum dynamics to be specified below. We introduce a highly nonlocal projective mapping as,

$$\begin{aligned} \tau_1^z &= \sigma_1^z P \\ \tau_{k \neq 1}^z &= \sum_{\vec{s}_k} \sigma_{k+\sum_{j=1}^{k-1} (s_j+1/2)}^z Q_{\vec{s}}^k P \end{aligned} \quad (1)$$

where the two projectors are

$$\begin{aligned} P &= \prod_{j=1}^{L-1} [1 - (\sigma_j^z + 1)(\sigma_{j+1}^z + 1)/4], \\ Q_{\vec{s}}^k &= \prod_{j=1}^{k-1} [s_j \tau_j^z + 1/2], \end{aligned} \quad (2)$$

with $\vec{s}_k = \{s_1, s_2, \dots, s_{k-1}\}$, $s_j = \pm 1/2$, $k \in [1, L_\tau]$, ($L_\tau \equiv L/2 + 1 - S_z$). Correspondingly, we have

$$\begin{aligned} \tau_k^+ \tau_{k'}^- & \\ &= \sum_{\vec{s}_k} \sigma_{k+\sum_{j=1}^{k-1} (s_j+1/2)}^+ Q_{\vec{s}}^k \sum_{\vec{s}'_{k'}} \sigma_{k'+\sum_{j=1}^{k'-1} s'_j+1/2}^- Q_{\vec{s}'_{k'}}^{k'} P, \end{aligned} \quad (3)$$

with $\sigma^\pm = (\sigma^x \pm i\sigma^y)/2$. These τ operators satisfy spin-1/2 algebra. Although the mapping appears a bit cryptic,

	Logical basis (f, τ)	Physical basis (c, σ)
Information	Preserved	Scrambled (hidden)
Basis-mapping	$\dots, 0011001\rangle, \dots$	$\dots, 001010001\rangle, \dots$
Hilbertspace Dimension	$\binom{L_\tau}{N}$	$\binom{L_\tau = L + 1 - N}{N}$
Hamiltonian	$H = \sum_k (f_k^\dagger f_{k+1} + H.c.)$	$H = P \sum_j (c_j^\dagger c_{j+1} + H.c.) P$
Operator growth	$f_k^\dagger f_{k'}$ remains quadratic	$c_j^\dagger c_{j'}$ becomes scrambled

TABLE I. The operator-mapping approach. In our designed framework, quantum information is stored in logical basis but scrambled in the physical basis. In the mapping from the logical to physical basis (both of which are represented by binary bit strings), we replace ‘0’ and ‘1’ by ‘0’ and ‘01’, respectively, then remove ‘0’ at the left-end to handle boundary effects. The mapping is bijective, and the Hilbert-space dimensions of the two basis are identical.

it becomes more explicit when looking at the transformation of eigenbasis of τ_z s and σ_z s. Taking an eigenstate of τ_z s, say $|0011001\rangle$, we first map each ‘0’ to ‘0’, and each ‘1’ to ‘01’, and then remove the left-most ‘0’. The transformed state is an eigenstate of σ_z s, with the example state mapped to $|001010001\rangle$ (see TABLE I). This mapping was previously used to study the ground-state Luttinger liquid [35, 36] and also excited-state many-body localization [37], but an operator form of the mapping was not known, and an efficient algorithm to calculate physical observables under the mapping was technically lacking—the calculation in the previous literature was consequently restricted to small system-sizes [36].

We shall consider a quantum state with information encoded as $\tau_k^z |\Psi\rangle = (2m_k^0 - 1) |\Psi\rangle$, that undergoes dynamical evolution according to the Hamiltonian

$$H = \frac{1}{2} \sum_{k=1}^{L_\tau} [\tau_k^x \tau_{k+1}^x + \tau_k^y \tau_{k+1}^y]. \quad (4)$$

An open boundary condition is adopted in this work. In the σ basis, the system is still local, and we have

$$H = \frac{1}{2} \sum_{j=1}^L P [\sigma_j^x \sigma_{j+1}^x + \sigma_j^y \sigma_{j+1}^y] P \quad (5)$$

and $\sigma_j^z |\Psi\rangle = (2n_j^0 - 1) |\Psi\rangle$. The eigenvalues m_k^0 and n_j^0 are related by the transformation-rule specified above.

The dynamics in this system is more transparent in the fermion picture through a Jordan-Wigner transformation, where we introduce f_k and c_j corresponding to τ and σ degrees of freedom, respectively. In the fermion picture, total S_z conservation implies that the total particle number $N (= S_z + L/2)$ is conserved. Corresponding to Eq. (4), f_k operators follow free fermion dynamics with a Hamiltonian $\sum_k (f_k^\dagger f_{k+1} + H.c.)$, and c_j follow dynamics of a spinless hard-core fermion model with infinite nearest neighbour interaction, whose ground state is shown to be an interacting Luttinger liquid [35, 36].

A sharp difference between the defined f_k and c_j operators is that in dynamical evolution, the operators $e^{-iHt} f_k^\dagger f_k e^{iHt}$ remain quadratic, whereas $e^{-iHt} c_j^\dagger c_j e^{iHt}$ necessarily involve many-body degrees of freedom, exhibiting operator growth. Consequently, dynamical operator $\sigma_j^z(-t)$ holding the information has a non-separable many-body character. Under this mathematical construction, the degrees of freedom τ and σ correspond to logical and physical basis, respectively. Properties of the mapping between the two are summarized in Table I.

Computation of the physical observables.— To make it more explicit, we have calculated such physical observables as Hamming distance, correlation relaxation, and out-of-time-order correlators, which confirm the operator growth and information scrambling in the high-complexity operator mapping approach. The results are provided in Supplementary Material. The late time dynamics shows a classical diffusion behavior—a classical description thus emerges despite the underlying quantum nature of microscopic degrees of freedom.

In the following, we analyze the computational complexity for the physical observables. For the dynamical quantum state, $|\Psi(t)\rangle = [F_k^\dagger(t)]^{m_k^0} |0\rangle$, the time-dependent wave function $\Psi_{\vec{m}}$ in the basis of $|\vec{m}\rangle = \prod_k [f_k^\dagger(0)]^{m_k} |0\rangle$ is a Slater-determinant. It is then straightforward to calculate the few-body observables in terms of the logical qubits via Wick theorem. However the Wick theorem does not carry over to observables composed of physical qubits. A direct calculation of the expectation value of such a physical observable \mathcal{O} , $\langle \mathcal{O} \rangle = \sum_{\vec{m}, \vec{m}'} \mathcal{O}_{\vec{m}\vec{m}'} \Psi_{\vec{m}}^*(t) \Psi_{\vec{m}'}(t)$, requires evaluating an exponentially large (in the system size) number of Slater-determinants, and is thus intractable for large systems. That problem actually restricts previous ground state calculations to very small system sizes [36]. To resolve this difficulty, we need an algorithm to sample the Slater determinants efficiently, which is provided below.

An efficient algorithm to sample Slater-determinant

wave-functions.— Here, we provide an explicit algorithm to sample the Slater determinants which do not require calculation of exponentially large number of determinants. This algorithm is inspired by a recent work on boson sampling which proposes a sampling method for permanents [38]. Considering a Slater-determinant state represented by a matrix U where each column represents a single-particle wave function. The algorithm contains three steps. The first step is to generate a random permutation of the integer sequence $[1, \dots, N]$, which has complexity $O(N)$. The generated sequence is denoted as a vector \vec{v} . The second step is to iteratively sample x_k (k is from 1 to N in the iteration) according to a conditional probability distribution

$$P(x_k | x_1, \dots, x_{k-1}; v_1, \dots, v_k) \propto \frac{1}{k!} |\text{Det}[U_{x_1 \dots x_k, v_1 \dots v_k}]|^2.$$

Then we choose an all zero vector \vec{m} and then set $m_{x_k} = 1$. The vector \vec{m} satisfies the required probability distribution $|\Psi_{\vec{m}}|^2$ because

$$\frac{1}{N!} \sum_{\vec{v}} \left[\prod_k P(x_k | x_1, \dots, x_{k-1}; v_1, \dots, v_k) \right] = |\Psi_{\vec{m}}|^2, \quad (6)$$

which follows from

$$\sum_{x_k} |\text{Det} U_{x_1 \dots x_k, v_1 \dots v_k}|^2 = \sum_{v \in [v_1 \dots v_k]} |\text{Det} U_{x_1 \dots x_{k-1}; [v_1 \dots v_k] \setminus v}|^2,$$

with $[v_1 \dots v_k] \setminus v$ keeping the elements in $[v_1 \dots v_k]$ except v . The sampling algorithm substantially improves the calculation efficiency compared to the previously used approach in studying ground state Luttinger liquids [36], and allows to treat much larger system sizes.

The major cost to calculate the physical observables arises from sampling the determinants. In the algorithm provided above, the complexity for M_s samples scales as $O(M_s L_\tau N^{z+1})$, with N^z the computational complexity to calculate the determinant of a $N \times N$ matrix ($z = 2.373$ with best known algorithm). Since the sampling error scales as $\varepsilon \sim 1/\sqrt{M_s}$, the computational complexity to calculate one physical observable is $O(\delta^{-2} L_\tau N^{z+1})$, with δ the required error threshold.

The overall computation complexity to calculate one physical observable is reduced to $O(L_\tau N^{3.373}/\delta^2)$ with δ the desired error threshold. The dynamics for the interacting physical system defined by the mapping (Eq. (1)) is thus *almost* exactly solvable, in the sense that the computational complexity does not scale exponentially.

We note here that the matrix elements of the dynamical many-body operator $\langle \vec{m} | e^{-iHt} c_j^\dagger c_j e^{iHt} | \vec{m}' \rangle$ holding the information in the physical basis, can also be calculated at a time cost which scales polynomially, much more efficient than the exponential scaling in conventional settings. All

details of the operator growth in the operator-mapping approach can thus be investigated efficiently with our method.

It is also worth emphasizing that the algorithm developed here is also a significant technical *advance* in solving hard-core fermion models, which allows for calculation of much larger system-sizes than previously accessible (comparing Supplementary Fig. S5 to results in Ref. 36). A straightforward variant of our algorithm could solve all finite-range interacting hard-core fermion models efficiently, details of which will be provided elsewhere.

We also emphasize that the algorithm we developed to sample the Slater-determinant wave functions can also be used to improve efficiency in other contexts. This explicit sampling algorithm is expected to accelerate variational Monte-Carlo calculations and improve quantum chemistry calculations. Our algorithm allows independent samplings that avoids the complication of autocorrelation in the commonly used Markov-chain sampling approach, thus improving the efficiency. Another application is to classically simulatable quantum machine learning [39] architectures by exploiting the quantum interference effects rather than the quantum computational power, which is of both fundamental and applicational importance.

Conclusion.— We have presented a novel mechanism for quantum information scrambling by hiding the information behind a highly nonlocal mapping, which relates the physical degrees of freedom to the logical ones holding the quantum information. A concrete operator mapping is provided to support this mechanism. We develop an algorithm to calculate physical observables, the complexity of which is polynomial in the system size. This allows us to simulate quantum dynamics of large systems. By calculating Hamming distance, correlation relaxation and out-of-time-order correlators in dynamics, we confirm the physical system exhibits quantum information scrambling and emergence of classical description at late time dynamics. We expect the proposed operator mapping approach to shed light on the fundamental understanding of information scrambling and quantum thermalization.

Acknowledgement.— We acknowledge helpful discussion with Yuan-Ming Lu, Meng Cheng, Lei Wang, and Sriram Ganeshan. This work is supported by National Program on Key Basic Research Project of China under Grant No. 2017YFA0304204 (XL), National Natural Science Foundation of China under Grants No. 117740067 (XL), and the Thousand-Youth-Talent Program of China (XL). G.Z. is supported by US ARO-MURI and US YIP-ONR. M.H. acknowledges support from the US National Science Foundation through grant PHY-1602867, and the Start-up Grant at Florida

Atlantic University, USA. X.W. acknowledges support from the Research Grants Council of the Hong Kong Special Administrative Region, China (No. CityU 11303617), the National Natural Science Foundation of China (No. 11604277), and the Guangdong Innova-

tive and Entrepreneurial Research Team Program (No. 2016ZT06D348). This work was completed at the Aspen Center for Physics, which is supported by US National Science Foundation Grant PHY-1607611.

-
- [1] Hammerer, K., Sørensen, A. S. & Polzik, E. S. Quantum interface between light and atomic ensembles. *Rev. Mod. Phys.* **82**, 1041–1093 (2010).
- [2] Duan, L.-M. & Monroe, C. Colloquium: Quantum networks with trapped ions. *Rev. Mod. Phys.* **82**, 1209–1224 (2010).
- [3] Georgescu, I. M., Ashhab, S. & Nori, F. Quantum simulation. *Rev. Mod. Phys.* **86**, 153–185 (2014).
- [4] Wendin, G. Quantum information processing with superconducting circuits: a review. *Reports on Progress in Physics* **80**, 106001 (2017).
- [5] Deutsch, J. M. Quantum statistical mechanics in a closed system. *Phys. Rev. A* **43**, 2046–2049 (1991).
- [6] Srednicki, M. Chaos and quantum thermalization. *Phys. Rev. E* **50**, 888–901 (1994).
- [7] Shaffer, D., Chamon, C., Hamma, A. & Mucciolo, E. R. Irreversibility and entanglement spectrum statistics in quantum circuits. *Journal of Statistical Mechanics: Theory and Experiment* **2014**, P12007 (2014).
- [8] Kaufman, A. M. *et al.* Quantum thermalization through entanglement in an isolated many-body system. *Science* **353**, 794–800 (2016). <http://science.sciencemag.org/content/353/6301/794.full.pdf>.
- [9] Gärtner, M. *et al.* Measuring out-of-time-order correlations and multiple quantum spectra in a trapped-ion quantum magnet. *Nature Physics* **13**, 781 EP – (2017).
- [10] Li, J. *et al.* Measuring out-of-time-order correlators on a nuclear magnetic resonance quantum simulator. *Phys. Rev. X* **7**, 031011 (2017).
- [11] Rigol, M., Dunjko, V. & Olshanii, M. Thermalization and its mechanism for generic isolated quantum systems. *Nature* **452**, 854 EP – (2008).
- [12] Poggi, P. M. & Wisniacki, D. A. Optimal control of many-body quantum dynamics: Chaos and complexity. *Phys. Rev. A* **94**, 033406 (2016).
- [13] Almheiri, A., Marolf, D., Polchinski, J. & Sully, J. Black holes: complementarity or firewalls? *Journal of High Energy Physics* **2013**, 62 (2013).
- [14] Roberts, D. A. & Swingle, B. Lieb-robinson bound and the butterfly effect in quantum field theories. *Physical review letters* **117**, 091602 (2016).
- [15] Gu, Y., Qi, X.-L. & Stanford, D. Local criticality, diffusion and chaos in generalized sachdev-ye-kitaev models. *Journal of High Energy Physics* **2017**, 125 (2017).
- [16] Chowdhury, D. & Swingle, B. Onset of many-body chaos in the o(n) model. *Physical Review D* **96**, 065005 (2017).
- [17] Patel, A. A., Chowdhury, D., Sachdev, S. & Swingle, B. Quantum butterfly effect in weakly interacting diffusive metals. *Physical Review X* **7**, 031047 (2017).
- [18] von Keyserlingk, C., Rakovszky, T., Pollmann, F. & Sondhi, S. Operator hydrodynamics, otocs, and entanglement growth in systems without conservation laws. *Physical Review X* **8**, 021013 (2018).
- [19] Nahum, A., Vijay, S. & Haah, J. Operator spreading in random unitary circuits. *arXiv preprint arXiv:1705.08975* (2017).
- [20] Chen, X., Fan, R., Chen, Y., Zhai, H. & Zhang, P. Competition between chaotic and nonchaotic phases in a quadratically coupled sachdev-ye-kitaev model. *Phys. Rev. Lett.* **119**, 207603 (2017).
- [21] Jian, S.-K. & Yao, H. Solvable sachdev-ye-kitaev models in higher dimensions: From diffusion to many-body localization. *Phys. Rev. Lett.* **119**, 206602 (2017).
- [22] Roberts, D. A., Stanford, D. & Streicher, A. Operator growth in the SYK model. *ArXiv e-prints* (2018). 1802.02633.
- [23] Shenker, S. H. & Stanford, D. Black holes and the butterfly effect. *JHEP* **03**, 067 (2014). 1306.0622.
- [24] Hayden, P. & Preskill, J. Black holes as mirrors: quantum information in random subsystems. *Journal of High Energy Physics* **2007**, 120 (2007).
- [25] Susskind, L. Black Holes and Complexity Classes. *ArXiv e-prints* (2018). 1802.02175.
- [26] Agón, C. A., Headrick, M. & Swingle, B. Subsystem Complexity and Holography. *ArXiv e-prints* (2018). 1804.01561.
- [27] Harlow, D. & Hayden, P. Quantum computation vs. firewalls. *Journal of High Energy Physics* **2013**, 85 (2013).
- [28] Maldacena, J. M. The Large N limit of superconformal field theories and supergravity. *Int. J. Theor. Phys.* **38**, 1113–1133 (1999). [Adv. Theor. Math. Phys.2,231(1998)], hep-th/9711200.
- [29] Sachdev, S. & Ye, J. Gapless spin-fluid ground state in a random quantum heisenberg magnet. *Physical review letters* **70**, 3339 (1993).
- [30] Kitaev, A. A simple model of quantum holography (2015).
- [31] Hauke, P. & Heyl, M. Many-body localization and quantum ergodicity in disordered long-range ising models. *Physical Review B* **92**, 134204 (2015).
- [32] Sekino, Y. & Susskind, L. Fast scramblers. *Journal of High Energy Physics* **2008**, 065 (2008).
- [33] Hastings, M. B. Locality in quantum systems. *Quantum Theory from Small to Large Scales* **95**, 171–212 (2010).
- [34] Lin, C.-J. & Motrunich, O. I. Out-of-time-ordered correlators in a quantum ising chain. *Phys. Rev. B* **97**, 144304 (2018).
- [35] Gómez-Santos, G. Generalized hard-core fermions in one dimension: An exactly solvable luttinger liquid. *Physical*

- review letters* **70**, 3780 (1993).
- [36] Cheong, S.-A. & Henley, C. L. Exact ground states and correlation functions of chain and ladder models of interacting hardcore bosons or spinless fermions. *Phys. Rev. B* **80**, 165124 (2009).
- [37] Li, X., Deng, D.-L., Wu, Y.-L. & Das Sarma, S. Statistical bubble localization with random interactions. *Phys. Rev. B* **95**, 020201 (2017).
- [38] Clifford, P. & Clifford, R. The classical complexity of boson sampling. In *Proceedings of the Twenty-Ninth Annual ACM-SIAM Symposium on Discrete Algorithms*, 146–155 (SIAM, 2018).
- [39] Biamonte, J. *et al.* Quantum machine learning. *Nature* **549**, 195 (2017).
-

Supplementary Material

S-1. HAMMING DISTANCE AS A MEASURE FOR INFORMATION SCRAMBLING

To explicitly show the information encoded in an initial product state of c_j operators would scramble into many-body degrees of freedom, we introduce a natural orbital bases $C_j(t)$ associated with c operators by diagonalizing the time-dependent correlation function by

$$\langle \Psi(t) | c_j^\dagger c_{j'} | \Psi(t) \rangle = \sum_i \lambda_i(t) U_{j,i}^c(t) U_{j',i}^{c*}(t), \quad (\text{S1})$$

and $C_i = \sum_j U_{j,i}^c c_j$. The natural orbital bases associated with f operators are defined in the same way as F_k , given by $F_k(t) = e^{-iHt} f_k e^{iHt}$.

To quantify information scrambling from few- to many-body degrees of freedom, we generalize a previously introduced Hamming distance [31] to natural orbital occupation basis. In this basis, the Hilbert space is spanned by the time-dependent states $|\vec{n}; t\rangle = [C_1^\dagger]^{n_1} [C_2^\dagger]^{n_2} \dots |0\rangle$. The Hamming distance that characterizes the distance between the dynamical state and the initial state in the Hilbert space is

$$\mathcal{D}(t) = \sum_{\vec{n}} (\vec{n} - \vec{n}_0)^2 |\langle \vec{n}; t | \Psi(t) \rangle|^2, \quad (\text{S2})$$

where \vec{n}_0 represents the initial occupation of natural orbitals. This Hamming distance is also a measure of *operator growth* [22]. The natural orbital basis is defined by sorting the eigenvalues λ_j in descending order, so that $\lambda_{j \leq N} = 1$, and $\lambda_{j > N} = 0$ for the initial state, and $\lambda_j \geq \lambda_{j+1}$ in general. For systems that do not exhibit information scrambling such as free fermions or many-body localized systems, $\mathcal{D}(t)$ remains to be an intensive quantity in dynamics, i.e., $\mathcal{D}(t)/L \rightarrow 0$, whereas $\mathcal{D}(t)/L$ becomes finite at long-time when the information spreads over the Hilbert space.

A direct calculation of the Hamming distance is still exponentially difficult. We thus rewrite it in terms of observables as

$$\mathcal{D}(t) = 2N \left[1 - \frac{1}{N} \sum_l n_{0,l} \lambda_l \right]. \quad (\text{S3})$$

Now the Hamming distance quantifying information spreading in the physical bases can be efficiently calculated at a polynomial time cost.

The results for Hamming distance are shown in Fig. S1. The information scrambling time t_S is determined by fitting the numerical results to $\mathcal{D}(t) = \mathcal{D}_\infty \arctan(t/t_S)$. We find that at long time limit \mathcal{D}_∞ is an extensive quantity, i.e., \mathcal{D}_∞/N is non-zero, and it approaches $2N(1 - \rho)$ as we increases total N , with the fermion density $\rho = N/L$. This means the quantum information encoded in the logical τ basis scrambles to the whole many-body Hilbert space in the σ basis. The scrambling time t_S , here referring to the time for the one-dimensional system to fully scramble, is found to have a $1/\rho$ dependence, which is qualitatively as expected because the effective interactions between physical fermions increase upon increasing the particle number density.

S-2. CORRELATION RELAXATION DYNAMICS

Apart from Hamming distance, the quantum memory loss in the physical basis can also be seen in the relaxation dynamics of correlations. Fig. S2 shows the evolution of the natural orbital occupation numbers, which are obtained through the eigenvalues of the correlation matrix $\langle \Psi(t) | c_i^\dagger c_j | \Psi(t) \rangle$. In the dilute limit of $\rho \rightarrow 0$, the interaction effects are vanishing, and the system is essentially formed by non-interacting fermions that do not relax. Away from that limit, we find efficient relaxation in the correlation, and the relaxation rate becomes stronger as we increase the particle number N . To quantify the relaxation dynamics, we introduce $Z(t) = \frac{1}{N} \sum_l \sqrt{\lambda_l(t)} \lambda_l(t \rightarrow \infty)$ that approaches 1 in the long-time limit.

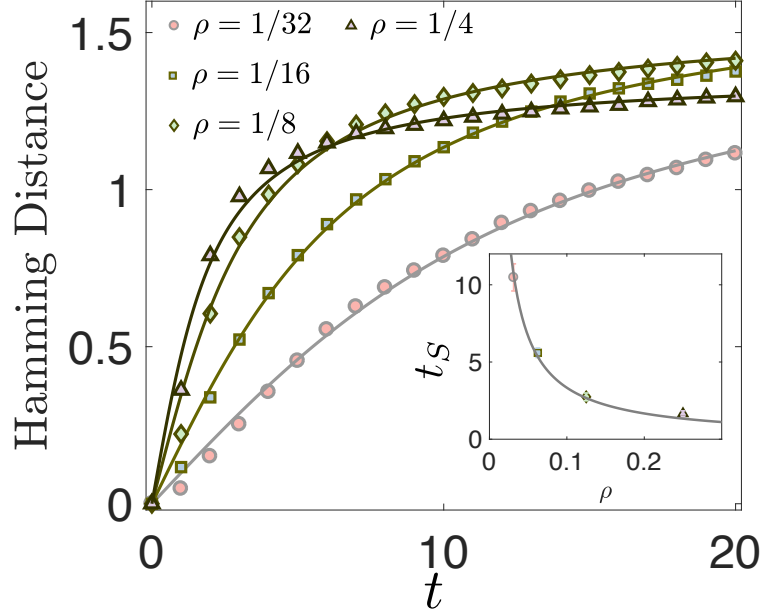


FIG. S1. Quantum information scrambling in Hilbert space measured by Hamming distance. In this figure, the shown Hamming distance is normalized by N . The system size is fixed to be 256 in this plot. We average over 10 random initial states and sampling 15000 states in Hilbert space to minimize the sampling error. The numerical results shown by symbol points fit to a function of $\arctan(t/t_S)$. The fitted form is shown by the lines in the plot. The characteristic time scale t_S exhibits a $1/\rho$ dependence as shown in the inset.

We find that for large systems the long-time behavior in $Z(t)$ is captured by $1 - Z(t) = \sqrt{t_r/t} + O(1/L)$, which is attributed to classical diffusive dynamics. At a time t much longer than microscopic time scales, the system is formed by domains of fermions in a vacuum background. The typical domain size is expected to be \sqrt{Dt} , with D the diffusion constant. The late-time behavior determined by the domain-size growth would lead to the $1/\sqrt{t}$ relaxation. This behavior also implies that a classical description could emerge from quantum many-body dynamics after the quantum information scrambles in the system.

The classical description consistent with numerical results is that at late time the particle density behaves as a classical superposition of localized domains, whose domain size grows according to the classical diffusion physics, i.e., $l_d = \sqrt{Dt}$, with D the diffusion constant. With the randomly distributed domains, the central limit theorem implies that the fermion density $\langle c_j^\dagger c_j \rangle$ satisfies a normal distribution with a mean N/L and variance $\text{Var} = N/L(l_d^{-1} - L^{-1})$. The average of $\sqrt{\langle c_j^\dagger c_j \rangle}$ is then given as

$$\sqrt{\langle c_j^\dagger c_j \rangle} = \sqrt{N/L} \left[1 - \frac{1}{8} \frac{\text{Var}}{(N/L)^2} \right] + O(1/L), \quad (\text{S4})$$

from which we get $1 - Z(t) \sim \sqrt{t}$, after substitution of l_d by \sqrt{Dt} .

S-3. OPERATOR-MAPPING ENABLED OTOC GROWTH

Despite the polynomial time cost in calculating all equal-time observables, our physical system still exhibits quantum chaotic behavior in the OTOC as in a generic thermalizing system to be explained below. The correlator we use here takes a form of $G_{jj'}(t) = \langle [\sigma_j^z(t), \sigma_{j'}^z(0)]^\dagger [\sigma_j^z(t), \sigma_{j'}^z(0)] \rangle_\beta$, with $\sigma_j(t)$ the Heisenberg operator, and $\langle \dots \rangle_\beta$ the thermal ensemble average. The sampling method we developed to calculate dynamics in few-body observables would breakdown in calculating OTOC at long time, because the sampling error would explode as $\sqrt{2^{3V_L t}/M_s}$, with M_s being

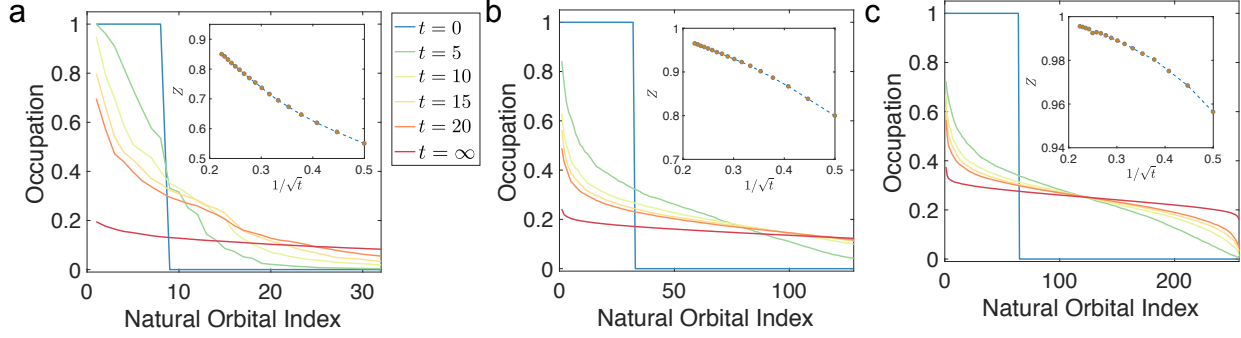


FIG. S2. Correlation relaxation dynamics of the physical degrees of freedom. (a, b, c) show the occupation numbers of natural orbital basis (see main text), with different $N = 8, 32, 64$, respectively. The total system size is fixed at $L = 256$. The $t = \infty$ results correspond to $t = 10^6$ in the calculation. Despite the logical degrees of freedom f_k are non-interacting, the physical ones show effective interaction effects in that natural orbital occupation exhibits relaxation behavior because otherwise they would not. The inset shows $Z(t)$ (see main text), which fits to a power law form of $1 - Z(t) = \sqrt{t_r/t} + O(1/L)$.

the sampling number, and v_L the Lieb-Robinson bound velocity. We thus evaluate OTOC with exact methods, and afford to simulate the dynamics up to a system size $L = 32$, with gpu techniques.

Figure S3 shows the results for OTOC where the exponential scrambling behavior of quantum information is observed. Effective interaction effects among the physical fermions are revealed as the OTOC spreading behaves as “ball-like” instead of “shell-like”, which differentiates interacting and free fermions [14]. This further confirms the information scrambling in this system. The early-time behavior of OTOC gives the Lyapunov exponent λ_L which exhibits a mild dependence of the temperature. Besides, the butterfly velocity is found to be approximately equal to the sound velocity in the conformal field theory at low energy, and its implication to black hole physics is worth further investigation.

Given that the physical system exhibits quantum chaotic behavior and that the computational complexity for simulating the quantum system is polynomial in the system size, our quantum operator-mapping scheme is expected to motivate further researches on the minimal microscopic computational complexity for chaotic phenomena, which is of fundamental interest in understanding complex many-body systems.

S-4. NUMERICAL VERIFICATION FOR THE SAMPLING METHOD

To show the convergence in the sampling of the natural orbital occupation, we provide the results with different total number of samplings M_s in Fig. S4. It is found that the results already converge with $M_s = 14000$, and that increasing to $M_s = 28000$ does not make noticeable difference. In the main text, we use $M_s = 15000$.

S-5. INTERACTION EFFECTS IN THE GROUND STATE

To show the interaction effects in the hard core fermion model, we provide the momentum distribution of the ground state in Fig. S5, which matches the interacting Luttinger liquid theory with Luttinger parameter $K < 1$. In the dilute limit, the momentum distribution approaches to the free fermion case. Increasing the density, the decrease of the Luttinger parameter implies the increase of effective interactions.

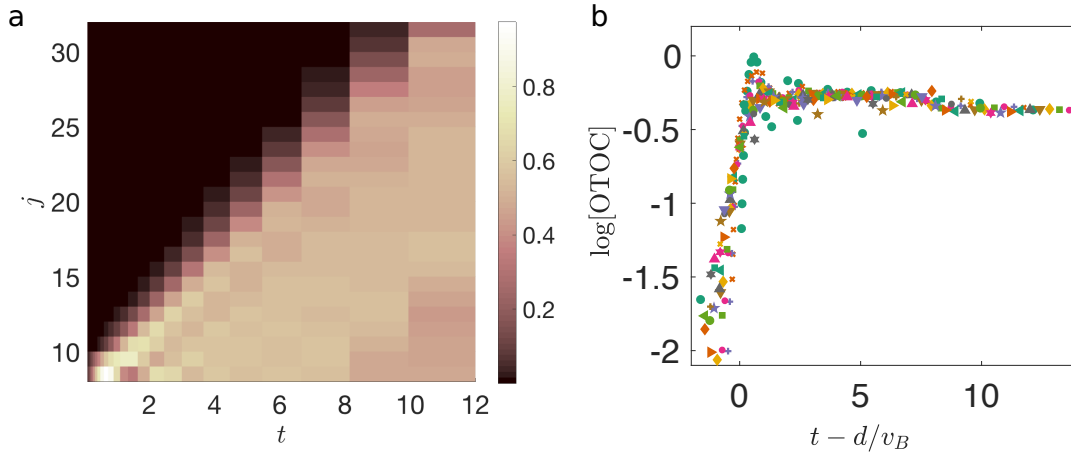


FIG. S3. Out-of-time-order correlator (OTOC) of the physical operators G_{ij} in dynamics. (a) shows the color plot of OTOC of $G_{i=8,j}$. In dynamics, the correlator exhibits a light-cone behavior with a finite butterfly velocity (v_B). Once the operator separation range in OTOC is within the light-cone, they quickly scramble and locally equilibrate. In this figure, the temperature is fixed to be 1 here. (b) shows the OTOC $G_{i=8,j}(t)$ versus $t - d/v_B$, with d the operator distance $d = j - 8$. Different symbols correspond to different j index. The OTOC early-time dynamics is consistent with an exponential growth. In the calculation we choose system size $L = 32$ and $N = 8$.

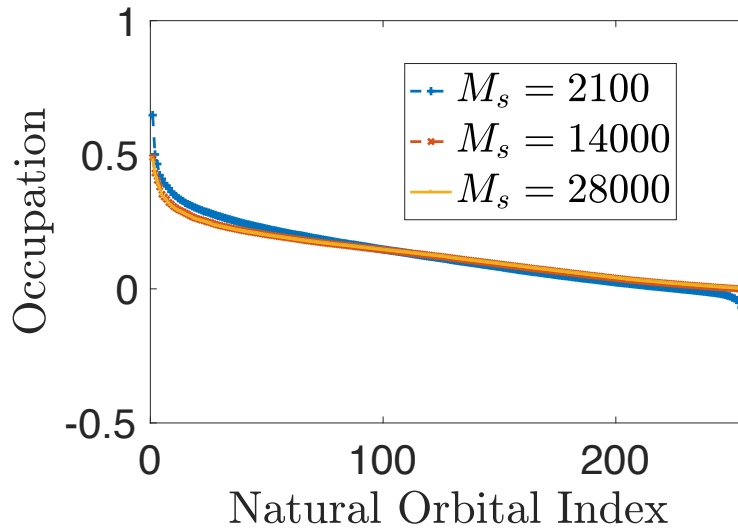


FIG. S4. Sampling convergence for the natural orbital occupation. This figure shows the natural orbital occupation at time $t = 20$ following the dynamics determined by the Hamiltonian in Eq. (2) starting from random initial states. From the results corresponding to different sampling number $M_s = 2100, 14000, 28000$, the results converge at the order of 10^4 .

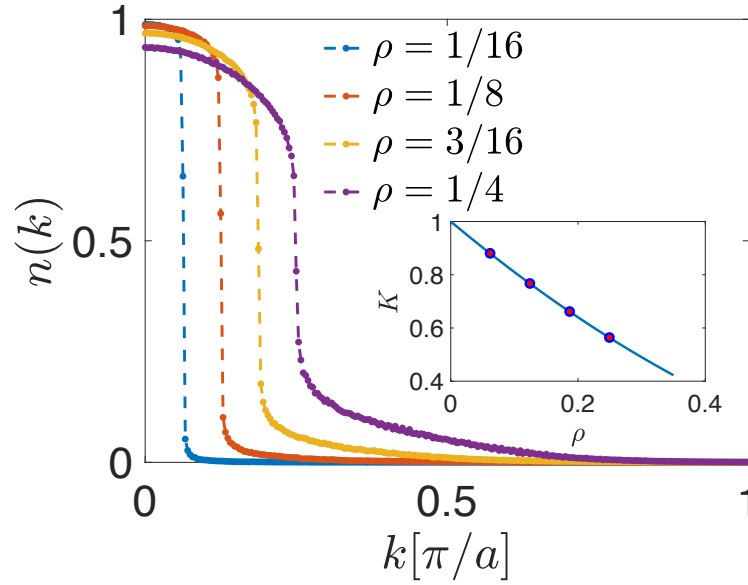


FIG. S5. Interaction effects in the model of hard-core spinless fermions. The momentum distribution $n(\mathbf{k})$ of the ground state is shown here, and it exhibits Luttinger liquid behavior. As we decrease the particle density, interaction effects become weaker, and the momentum distribution is approaching fermi-surface type. The interaction effects in this model can also be quantified by the deviation of the the ground state luttinger parameter K from the fermion case which has $K = 1$ (see the inset). The number of lattice sites used here is $L = 512$.